

# Journal of Materials Chemistry C

Accepted Manuscript



This is an *Accepted Manuscript*, which has been through the Royal Society of Chemistry peer review process and has been accepted for publication.

*Accepted Manuscripts* are published online shortly after acceptance, before technical editing, formatting and proof reading. Using this free service, authors can make their results available to the community, in citable form, before we publish the edited article. We will replace this *Accepted Manuscript* with the edited and formatted *Advance Article* as soon as it is available.

You can find more information about *Accepted Manuscripts* in the [Information for Authors](#).

Please note that technical editing may introduce minor changes to the text and/or graphics, which may alter content. The journal's standard [Terms & Conditions](#) and the [Ethical guidelines](#) still apply. In no event shall the Royal Society of Chemistry be held responsible for any errors or omissions in this *Accepted Manuscript* or any consequences arising from the use of any information it contains.

## COMMUNICATION

## Chip-based microcavity derived from multi-component tellurite glass

Cite this: DOI: 10.1039/x0xx00000x

Binbin Zheng,<sup>a</sup> Mingxiao Zhao,<sup>b</sup> Qiangbing Guo,<sup>a</sup> Yongze Yu,<sup>c</sup> Shichao Lv,<sup>c</sup> Xiaoshun Jiang<sup>b\*</sup> and Shifeng Zhou<sup>a, c, \*</sup>Received 00th January 2012,  
Accepted 00th January 2012

DOI: 10.1039/x0xx00000x

www.rsc.org/

**Construction of chip-based optical microcavity from multi-component glass has long been a significant fundamental challenge in the cross field of materials science and photonics. Here we introduced a scalable non-hydrolytic sol-gel method for deposition of multi-component glass film with high thickness and superior homogeneity. Prototypically, we demonstrated the success in fabrication of multi-component tellurite thick film, and construction of tellurite microcavity on silicon chip through a combined etching technology for the first time. The collaborative studies by using steady-state spectrum, whisper gallery mode (WGM) resonance spectrum and electric field distribution firmly indicate that the obtained thick film and microcavity present excellent properties, point to the promising application in integrated photonics.**

### Introduction

Chip-based optical microcavity has attracted much attention, owing to its excellent light management capability for a broad range of applications, such as high-density data storage, low-threshold laser, and biological sensing.<sup>1-5</sup> To date, most effort has focused on the glassy silica derived microcavity, mainly because of the mature technology for fabrication of low-loss silica glass with high durability.<sup>6-8</sup> On the other hand, multi-component glass represents another particularly attractive system for photonic applications owing to the exceptional properties, including high optical nonlinearity, optimized chromatic dispersion, and high rare-earth ion solubility.<sup>9,10</sup> Thus, it was believed to be a promising material candidate for the next generation microcavity device. Unfortunately, it still remains a grand challenge for construction of multi-component glass based microcavity on a chip.

In this letter, we introduce a scalable approach, based upon non-hydrolytic sol-gel (NHSG) process, for deposition of thick tellurite glass film with high homogeneity. We then demonstrate that the reliable thick film can be further fabricated into microcavity on silicon. To the best of our knowledge, the progress provides the first prototype of chip-based optical microcavity derived from multi-component glass.

### Experimental

Tellurium dioxide (TeO<sub>2</sub>), 1,2-propanediol (C<sub>3</sub>H<sub>6</sub>(OH)<sub>2</sub>) and p-toluene sulfonic acid were mixed (mole ratio = 1:8:0.1) in a glass flask and the mixture was stirred and heated at 140 °C for 6 h until the white TeO<sub>2</sub> particles disappeared. Then, the hot clear solution was filtered to remove the by-product such as metal tellurium. After held at room temperature for several days, a large quantity of Te-alkoxide crystalline, Te(O<sub>2</sub>C<sub>3</sub>H<sub>6</sub>)<sub>2</sub>, precipitated from the solution. Subsequently, the alkoxide products were collected by filtration and dried at room temperature in vacuum drying oven. Finally, the Te(O<sub>2</sub>C<sub>3</sub>H<sub>6</sub>)<sub>2</sub> precursor was dissolved into 1,2-propanediol to obtain 1 mol/L Te(O<sub>2</sub>C<sub>3</sub>H<sub>6</sub>)<sub>2</sub> precursor solution.

The homogeneous tellurite sol was prepared by non-hydrolytic sol-gel method with a composition of (mol%) 80TeO<sub>2</sub>-10ZnO-10Na<sub>2</sub>O. The required quantities of Zn(CH<sub>3</sub>COO)<sub>2</sub> and CH<sub>3</sub>COONa were added into 1,2-propanediol and stirred at 60 °C for 2 h. Then, the mixed solution was added into the obtained Te(O<sub>2</sub>C<sub>3</sub>H<sub>6</sub>)<sub>2</sub> precursor solution and refluxed at 80 °C for 2 h to gain transparent sol. Yb(CH<sub>3</sub>COO)<sub>3</sub> and Er(CH<sub>3</sub>COO)<sub>3</sub> were additionally introduced into the solution for obtaining co-doped tellurite sol.

The tellurite sol was deposited onto silicon chip by spin-coating method with a spin speed of 2000 rpm for 20 s, followed by preheat-treatment at 80 °C for 12 h and then annealed at 300 °C for 2 h with an annealing rate of 0.5 °C/min. The thickness of single layer was approximately 100 nm, and the required ~1 μm film for microcavity was prepared after 10 cycles of spin-coating and anneal step.

The tellurite microdisk cavity with diameter of 80 μm was created on silicon chip through a combination method of photolithography, buffered HF etching and SF<sub>6</sub> dry-etching. In detail, the standard photolithography was performed to create circular photo-resist pad (80 μm in diameter) on silicon chip coated with thick tellurite film. Tellurite layer was corroded by immersing the sample into buffered HF solution with a composition of 3 ml HF: 6 g NH<sub>4</sub>F: 10 ml H<sub>2</sub>O for 20 min. Then, the chip was washed by acetone and isopropanol for twice for removing photo-resist and residual organic contamination. The silicon substrate was isotropically etched by SF<sub>6</sub> gas at 2 torr for 40 min, which was carried out in a plasma etching (PE) semiconductor equipment.

The XRD pattern was performed on a RIGAKU D/MAX 2550/PC diffractometer with Cu K $\alpha$  radiation. The Raman spectrum was determined by a LabRam HRUV Laser Raman spectrophotometer. The morphology of tellurite microdisk cavity was characterized by Scanning Electron Microscopy (SEM, Hitachi S4800) and Atomic Force Microscopy (AFM, Veeco MultiMode). The emission (PL) spectra were measured using an FLS920 fluorescence spectrophotometer.

The optical resonance simulation by the finite difference time domain (FDTD) method was performed using commercial software (FDTD Solutions, Lumerical Solutions, Canada). In the simulation, mode light at  $\sim 1550$  nm was employed as input light. The calculations were performed on a cubic grid having a discretization step of small enough, with perfectly matched layer (PML) conditions imposed at the boundaries.

## Results and discussion

The optimized synthesis of precursor sol with high homogeneity is vital in order to fabricate thick film with excellent properties. In conventional hydrolytic sol-gel (HSG) process, it is difficult to coordinate hydrolysis and condensation kinetics of the precursor sol, thus always giving rise to inhomogeneous micro-structure and macroscopically non-transparent appearance of the deposited film. As a typical example, Fig. 1a shows the schematic structure of tellurium alkoxide precursor which is frequently used for fabrication of multi-component glass.<sup>11</sup> There are two lone pair electrons (LPE) around tellurium atom, thus leaving a large open space to be occupied by H<sub>2</sub>O and facilitating induced weakening of Te-O covalent bond. The weak steric effect for oxygen donors (OD) would dramatically accelerate hydrolysis process. As a result, the condensation process cannot keep pace with hydrolysis process and undesirable precipitation of crystalline TeO<sub>2</sub> will occur before formation of long-range network, leading to the sharp reduction in film forming capability.

In order to circumvent these sticky issues, we proposed a non-hydrolytic (NHSG) pathway by using alkoxide precursor for the purpose of modulating reaction kinetic of sol-gel process. Specifically, we designed a novel tellurium alkoxide (Te(O<sub>2</sub>C<sub>3</sub>H<sub>6</sub>)<sub>2</sub>) with the unique stereo configuration of tellurium atom surrounded by branched alkyl groups (Fig. 1b). In this structure, the sol-gel process is expected to start with the heterolytic cleavage of O-C bonds and LPE-induced weakening of Te-O bonds in tellurite precursor. Then, the liberated alkyl cations connect with the adjacent terminal alkoxide groups to form C-O-C bonds and meanwhile the Te-O-Te bonds become stronger. Finally, the chainlike molecular clusters are cross-linked together till stable network formed (Fig. 1c). Another intriguing feature of the proposed NHSG strategy is that the other important modifiers such as Zn<sup>2+</sup> and Na<sup>+</sup> can be conveniently introduced into sol system without loss of homogeneity, which is in stark contrast to the conventional HSG process, where the tellurium precursor and the other precursor species always show significantly great mismatch of hydrolysis rates, thus applicable for fabrication of thick film.<sup>12</sup>

As a proof-of-concept experiment, we firstly synthesized Te(O<sub>2</sub>C<sub>3</sub>H<sub>6</sub>)<sub>2</sub> precursor by alcoholization reaction between TeO<sub>2</sub> and 1,2-propanediol that was catalyzed with p-toluene sulfonic acid (PTSA). By using the obtained product, we then tried to fabricate homogeneous multi-component tellurite sol with the composition of (mol%) 80TeO<sub>2</sub>-10ZnO-10Na<sub>2</sub>O. Benefiting from the steric effect of the branched alkyl groups in Te(O<sub>2</sub>C<sub>3</sub>H<sub>6</sub>)<sub>2</sub> precursor, the whole NHSG process can be well designed and optimized to a suitable rate. The additionally introduced Zn<sup>2+</sup> and Na<sup>+</sup> are expected to fill a fraction of occupied space of LPE sites in the structural units of TeO<sub>2</sub>, further facilitating the formation of strong tellurite network.

Worthy to note, compared to conventional sol-gel route, NHSG method has another advantage that it can occur without the participation of H<sub>2</sub>O, which not only helps to avoid stringent control over a set of experimental variables, such as pH value, concentration of metal precursors, but also prevents the undesirable optical loss induced by -OH groups. As a result, the highly homogeneous multi-component tellurite sol was fabricated, confirmed by the Tyndall test as shown in Fig. 1d and Fig. 1e, suggesting the success in modulating NHSG route with optimized precursor.

Tellurite film was then fabricated by depositing the obtained sol onto a commercial silicon chip by spin-coating method. In this work, we chose 1,2-propanediol as the solvent because it possesses high viscosity and relatively high boiling point, which not only increases the steric effect, but also avoids unexpected capillary force. Especially, the significant decrease of capillary force between tellurite layers is highly beneficial for construction of thick film. As an example shown in Fig. 2a, the thick film with uniform morphology can be well kept in the crack-free state even after heat-treatment at 300 °C for 2 h. From the cross-sectional SEM image of tellurite film shown in Fig. 2b, the thickness was estimated to be  $\sim 1$   $\mu$ m and it is necessary to note that the inner structure is extremely dense, which provides great convenience for the subsequent microcavity fabrication.

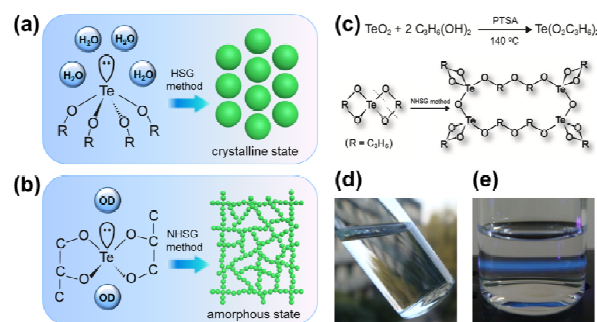


**Fig. 1** (a) and (b) Schematic structures of conventional tellurium alkoxide precursor and optimized Te(O<sub>2</sub>C<sub>3</sub>H<sub>6</sub>)<sub>2</sub> precursor and the resultant sol-gel products. (c) Synthesis route for fabrication of Te(O<sub>2</sub>C<sub>3</sub>H<sub>6</sub>)<sub>2</sub> precursor and tellurite glass. (d) The appearance of homogeneous tellurite sol. (e) Tyndall test of the synthesized tellurite sol.

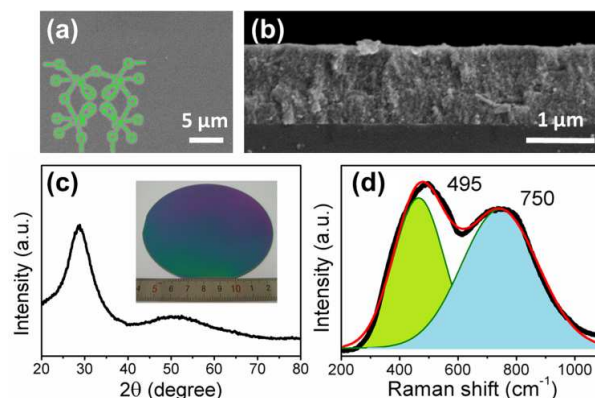


**Fig. 2** (a) SEM image of tellurite thick film. Inset: schematic structure of tellurite network. (b) Cross-sectional SEM image of thick tellurite film with a thickness of  $\sim 1$   $\mu$ m. (c) XRD pattern of tellurite film. Inset: photograph of tellurite film on a silicon chip. (d) Raman spectrum of tellurite film.

The structure features of the obtained film were collaboratively studied by using X-ray diffraction (XRD) and Raman spectrum. A broadband halo can be observed in the XRD spectra (Fig. 2c), indicating the amorphous nature of tellurite film; This confirms the success in modulating reaction kinetic of NHSG process. Raman spectrum (Fig. 2d) provides the valuable information about the network structure of amorphous tellurite film. The broad peak at  $495\text{ cm}^{-1}$  is originated from Te-O-Te linkages and the peak of  $750\text{ cm}^{-1}$  should be attributed to  $\text{TeO}_4$  bi-pyramidal units and  $\text{TeO}_3$  pyramidal units.<sup>13</sup> From Raman spectrum, the maximum phonon energy of the thick film can be estimated to be  $\sim 750\text{ cm}^{-1}$ , which is relative low, thus making it potential to achieve high luminescence efficiency after incorporation of various types of rare earth ions.

The first key advantage of the obtained reliable and thick tellurite film is that it enables the construction of novel on-chip photonic structure. To test it, we further carried out the fabrication of optical microcavity on the surface of silicon with the combinative photolithography and etching method. The standard photolithography was performed to create circular photo-resist pad ( $80\text{ }\mu\text{m}$  in diameter) on silicon chip coated with thick tellurite film. When the sample was immersed into buffered HF solution, the photo-resist acted as an etch mask and the exposed tellurite layer was corroded (Fig. 3b and Fig. 3f). Subsequently, acetone and isopropanol were adopted to remove the photo-resist and residual organic contamination (Fig. 3c). Importantly, the tellurite disk with smooth edge and uniform surface can be obtained, as shown in Fig. 3g. Finally, the chip was exposed to  $\text{SF}_6$  gas for the purpose of isotropically selective removal of silicon, resulting in the prominence of disk-shape tellurite microcavity upon a silicon pillar (Fig. 3d and Fig. 3h). The surface roughness of the fabricated structure was studied with AFM and it was estimated to be around  $8\text{ nm}$ . To the best of our knowledge, the results presented above demonstrated the first success in construction of chip-based microcavity derived from multi-component tellurite glass.

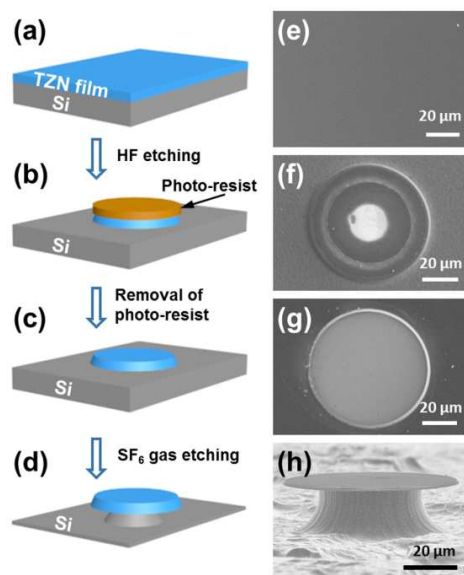


**Fig. 3** Fabrication process of microcavity from from multi-component tellurite glass.

The second key advantage of the constructed thick film and derived microcavity consists of the essentially homogeneous multi-component tellurite in perfectly amorphous state. This enables the rational incorporation of various active dopants with negligible clustering, which is not feasible in the conventional single component glass system such as silica.<sup>14</sup> As a proof-of-concept

experiment, erbium ( $\text{Er}^{3+}$ ) and ytterbium ( $\text{Yb}^{3+}$ ) were selected as dopants, taking into account their fundamental roles in active photonics. It is significant to find that even in the case of extremely heavy doping (10%  $\text{Yb}^{3+}$  and 5%  $\text{Er}^{3+}$ ), the radiative transitions from active dopants can still be clearly observed. As shown in Fig. 4a, under excitation with a 980 nm diode laser, the distinct up-conversion emission bands at 410, 526, 548, and 660 nm can be well indexed to  ${}^2\text{H}_{9/2} \rightarrow {}^4\text{I}_{15/2}$ ,  ${}^2\text{H}_{11/2} \rightarrow {}^4\text{I}_{15/2}$ ,  ${}^4\text{S}_{3/2} \rightarrow {}^4\text{I}_{15/2}$ , and  ${}^4\text{F}_{9/2} \rightarrow {}^4\text{I}_{15/2}$  transitions of  $\text{Er}^{3+}$ , respectively (Fig. 4c). In addition, a broad near-infrared (NIR) emission at  $\sim 1535\text{ nm}$  was also observed and the full width at half maximum (FWHM) was estimated to be  $\sim 69\text{ nm}$  (Fig. 4b) which is as about twice as that of Er-doped single component materials.<sup>15</sup> In notable contrast to conventional active materials, the structure shown here provides a multitude of advantages, including multi-color emission covering the whole red-green-blue (RGB) region, broadband NIR emission and much high nonlinear refractive index ( $\sim 40 \times 10^{-19}\text{ m}^2\text{ W}^{-1}$ ). Thus, it should be noted that utilization of the developed structure is promising to enable the development of the next generation compact microcavity device with unprecedented capability of tunable emission and optical switching.

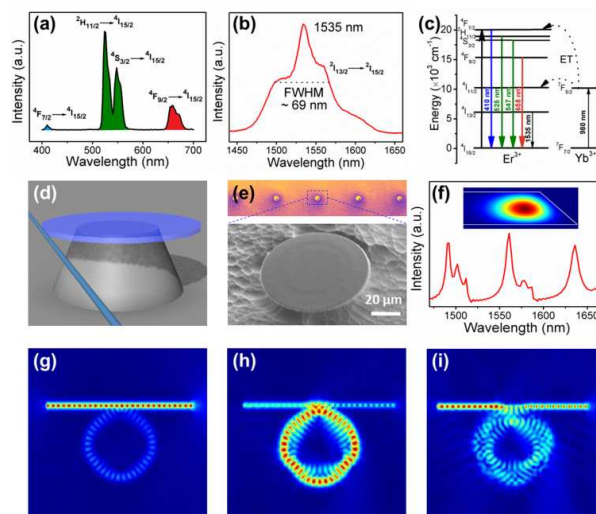


**Fig. 4** (a) Up-conversion emission bands of tellurite microcavity with 980 nm laser. (b) NIR emission signal of tellurite microcavity with 980 nm laser. (c) Schematic energy level diagram of  $\text{Yb}^{3+}$  and  $\text{Er}^{3+}$  ions. (d) Schematic diagram of tellurite microcavity as optical resonator. (e) SEM images of tellurite microcavity array and a single microcavity. (f) Resonant spectrum in tellurite microcavity with a fiber taper coupling configuration. Inset: cross-sectional mode distribution of the tellurite microcavity with an angled sidewall. (g-i) Mode distributions of TE field in the equatorial plane of the tellurite microcavity at different coupling condition: undercoupling (g), best coupling (h) and overcoupling (i).

The successful construction of chip-based microcavity with well-defined shape and ultra-smooth edge suggests the potential application in integrated photonics. For example, Fig. 4d depicts the schematic diagram of the tellurite microcavity as optical resonator operated on the whisper gallery mode (WGM). A fiber taper was employed for the purpose of evanescently coupling of light into or out the tellurite microcavity. The simulated resonance spectrum clearly indicates that the WGM resonance can be achieved on the constructed tellurite microcavity (Fig. 4e and Fig. 4f). Furthermore, the distribution of transverse electric (TE) field in the equatorial plane was also investigated and the results demonstrate that on the condition of the best coupling, the light with the wavelength of  $\sim 1550\text{ nm}$  can efficiently propagate along the cavity-surrounding

interface via total internal reflection (Fig. 4g-i). The results confirm the robust photon-management capability with long intra-cavity photon lifetime and strong light confinement in the fabricated tellurite microcavity.

### Conclusions

In conclusion, we have introduced a scalable approach for fabrication of multi-component glass film with high homogeneity, enabled by the success in modulating the reaction kinetics of non-hydrolytic sol-gel process. Accordingly, amorphous tellurite film with large thickness and chip-based microcavity with smooth edge and uniform surface were successfully constructed, and then demonstrated to potentially present excellent optical performance. Our results provide the first prototype of chip-based optical microcavity derived from multi-component glass and pave the way to develop the next generation compact microcavity device.

### Acknowledgements

The authors gratefully acknowledge the financial support from the National Natural Science Foundation of China (Grant. 11474102), the Chinese Program for New Century Excellent Talents in University (Grant NCET-13-0221), Guangdong Natural Science Funds for Distinguished Young Scholar (Grant S2013050014549), and the Scientific Research Foundation for Returned Overseas Chinese Scholars, State Education Ministry.

### Notes and references

<sup>a</sup> State Key Laboratory of Silicon Materials, School of Materials Science and Engineering, Zhejiang University, Hangzhou 310027, China. E-mail: zhoushifeng@scut.edu.cn; Fax: +86 57188925079; Tel: +86 57188925079.

<sup>b</sup> National Laboratory of Solid State Microstructures and College of Engineering and Applied Sciences, Nanjing University, Nanjing 210093, China. E-mail: jxs@nju.edu.cn

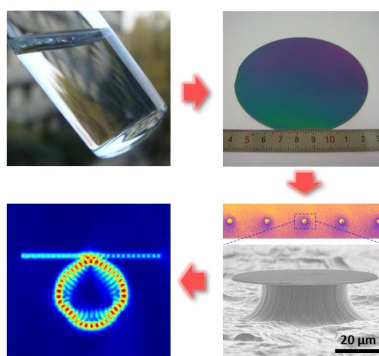
<sup>c</sup> State Key Laboratory of Luminescent Materials and Devices, Institute of Optical Communication Materials, South China University of Technology, Guangzhou 510640, China.

† Electronic Supplementary Information (ESI) available: [details of any supplementary information available should be included here]. See DOI: 10.1039/c000000x/

- 1 J. Li, X. Yi, H. Lee, S. A. Diddams, and K. J. Vahala, *Science*, 2014, **345**, 309.
- 2 L. Shao, X. Jiang, X. Yu, B. Li, W. R. Clements, F. Vollmer, W. Wang, Y. Xiao, and Q. Gong, *Adv. Mater.*, 2013, **25**, 5616.
- 3 D. K. Armani, T. J. Kippenberg, S. M. Spillane, and K. J. Vahala, *Nature*, 2003, **421**, 925.
- 4 L. Yang, T. Carmon, B. Min, S. M. Spillane, and K. J. Vahala, *Appl. Phys. Lett.*, 2005, **86**, 091114.
- 5 G. Wang, X. Jiang, M. Zhao, Y. Ma, H. Fan, Q. Yang, L. Tong, and M. Xiao, *Opt. Express*, 2012, **20**, 29472.
- 6 F. Bo, S. H. Huang, S. K. Özdemir, G. Zhang, J. Xu, and L. Yang, *Opt. Lett.*, 2014, **39**, 1841.
- 7 H. Li, L. Shang, X. Tu, L. Liu, and L. Xu, *J. Am. Chem. Soc.*, 2009, **131**, 16612.
- 8 L. Chang, X. Jiang, S. Hua, C. Yang, J. Wen, L. Jiang, G. Li, G. Wang, and M. Xiao, *Nat. Photonics*, 2014, **8**, 524.

- 9 A. Jha, B. Richards, G. Jose, T. Teddy-Fernandez, P. Joshi, X. Jiang, and J. Lousteau, *Prog. Mater. Sci.*, 2012, **57**, 1426.
- 10 L. Zhang, J. C. C. Chan, H. Eckert, G. Hensch, L. P. Hoyer, and G. H. Frischat, *Chem. Mater.*, 2003, **15**, 2702.
- 11 L. Weng, and S. N. B. Hodgson, *J. Non-Cryst. Solids*, 2002, **297**, 18.
- 12 L. Weng, and S. N. B. Hodgson, *Opt. Mater.*, 2002, **19**, 313.
- 13 J. Jackson, C. Smith, J. Massera, C. Rivero-Baleine, C. Bungay, L. Petit, and K. Richardso, *Opt. Express*, 2009, **17**, 9071.
- 14 L. He, S. K. Özdemir, and L. Yang, *Laser Photonics Rev.*, 2013, **7**, 60.
- 15 M. Fukushima, N. Managaki, M. Fujii, H. Yanagi and S. Hayashi, *J. Appl. Phys.*, 2005, **98**, 024316.

## Table of Contents



Our results provide the first prototype of chip-based optical microcavity derived from multi-component tellurite glass.